Particle effects on friction and wear of aluminium matrix composites

Z. F. ZHANG, L. C. ZHANG*, Y.-W. MAI
Centre for Advanced Materials Technology, Department of Mechanical and Mechatronic Engineering, University of Sydney, Sydney 2006, Australia

Particle effects on friction and wear of 6061 aluminium (6061 Al) reinforced with silicon carbide (SiC) and alumina (Al_2O_3) particles were investigated by means of Vickers microhardness measurements and scratch tests. Unreinforced 6061 Al matrix alloy was also studied for comparison. To explore the effect of heat treatment, materials subjected to three different heat treatment conditions, i.e. under-aged, over-aged and T6, were used. Multiple-scratch tests using a diamond and a steel indentor were also carried out to simulate real abrasive wear processes. Vickers microhardness measurements indicated that T6 heat-treated composites had the highest hardness. Single-scratch tests showed that the variation of friction coefficient was similar to that of Vickers hardness and the peak-aged composites exhibited the best wear resistance. The wear rate of fine particle-reinforced composites was mainly affected by hardness. However, the wear rate of large particle-reinforced composites was influenced by both the hardness and fracture of the particles.

1. Introduction

The wear behaviour of particle-reinforced aluminum matrix composites has been investigated extensively in the past 10 years owing to their promising wear resistance [1–7]. Previous studies have shown that abrasive wear resistance of composites strongly depends on their hardness and also relates to the particle volume fraction and size [1, 2, 6]. Some authors studied the ageing effect on wear of these composites and indicated that different ageing conditions could result in varied wear behaviour. For example, Wang and Rack [1], Ma *et al.* [2] and Lin and Liu [6] showed that peak-aged aluminium composites had the best wear resistance compared to other ageing conditions when sliding against abrasive papers. On the contrary, Alpas and Embury [7] indicated a decreased wear resistance with increasing hardness when sliding against metals, implying that the counterface could play an important role. In addition, wear tests on different heat-treated steels showed that the wear resistance increased slowly with increasing hardness [8]. Although a series of studies has been done and several wear models proposed [1, 8–11], the understanding of friction and wear behaviour is far from complete. This work aimed to understand, with the aid of hardness and scratch tests, the behaviour of friction and wear of metal matrix composites, in terms of particle sizes and ageing conditions.

2. Experimental procedure

The materials tested were 6061 Al matrix alloy and its composites reinforced by 10 and 20 vol% angular shaped SiC and Al_2O_3 particles (Duralcan). The average diameters were 1.8 μm for SiC particles and 4.5 μm (10% reinforcement) and 8.8 μm (20% reinforcement) for Al_2O_3 particles. The materials were supplied by Comalco Pty Ltd, Australia. A composite of 20 vol% spherical alumina with an average diameter of 18.7 μm (Comral-85) was also studied. The matrix alloy composition of Comral-85 was different to that of Duralcan. To explore the effect of heat treatment, three conditions of heat treatment, (1) underaged (1.5 h solution treatment at 530 °C, quenching into water followed by natural ageing for 20 h and then artificially aged at 175 °C for 2 h), (2) overaged (artificial ageing at 175 °C for 20 h), and (3) T6 condition (artificial ageing at 175 °C for 8 h), were investigated for all the materials used in this study. As the particle sizes and volume fractions varied over a wide range, Vickers microhardness was measured for all the materials at a load of 5 N.

Wear tests were carried out on a scratch wear machine. Detailed description of the experimental methods can be found elsewhere [3]. For the present study, a pyramidal diamond indentor with an apex angle 2θ equal to 136° was used in both single and multiple scratches. The orientation of the indentor was taken with one leading plane moving forward during scratching. A steel cone indentor with the same apex angle of 136° was also used for multiple scratches. A velocity of 6 mm s^{-1} was used over a wear track about 6 mm and the applied load was 10 N.

* Author to whom all correspondence should be addressed.

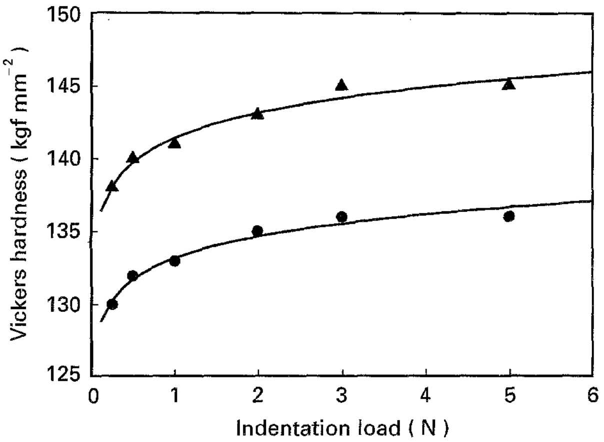

Figure 1 Dependence of Vickers hardness on the indentation load for 20% Al_2O_3–Al composites: (●) spherical, (▲) angular.

3. Results and discussion

3.1. Vickers microhardness tests

It is well known that the hardness of a material is a major wear parameter in Archard's wear equation [12]. For a particle-reinforced composite, however, the microhardness may vary over a wide range, because the indentor may be placed at either the matrix area or the area of a cluster of particles, depending on the particle size and volume fraction, and the magnitude of the indentation load. To explore the hardness and particle effects on the friction and wear, different hardness values were achieved by different heat treatments. Because of the large particle sizes, the Vickers hardness of Al_2O_3–Al composites increases with increasing indentation load, as shown in Fig. 1. The hardness of a particle-reinforced composite is usually determined by averaging a series of measured hardness values under an appropriate indentation load. In general, the Vickers hardness, H, depends on the matrix hardness, H_m, the particle hardness, H_p, particle volume fraction, f_v, particle size, d, the indentation load, P, and ageing condition. Thus, the Vickers hardness is a function of these parameters, i.e.

$$H = f(H_m, f_v, d, H_p, P, g) \quad (1)$$

where g is a factor reflecting the effect of ageing conditions.

Based on the results of the hardness test, see Table I and Fig. 1, a practical non-dimensional equation for the present particle-reinforced composites can be expressed as

$$\bar{H} = 1 + g f_v^{1.8} \bar{H}_p^{0.4} \bar{P}^{0.1} \quad (2)$$

where $\bar{H} = H/H_m, \bar{H}_p = H_p/H_m, \bar{P} = P/(H_m d^2)$, and g is 0.77, 0.58 and 0.50 for Duralcan composites at T6, overaged and underaged conditions, respectively. The hardness of SiC is 2480 kgf mm^{-2} and that of Al_2O_3 is 2100 kgf mm^{-2}. The Vickers matrix hardness values at T6, over-aged and under-aged conditions are 120, 108 and 102 kgf mm^{-2}, respectively, at the same indentation load of 5 N. It should be noted that the Vickers hardness of SiC–Al composites is almost independent of indentation load, because of the reinforced SiC particles are so fine (less than 2 μm) that the indenting area always covers several particles and more or less the same hardness value can be obtained. Therefore, an indentation load of 5 N is used for this kind of fine particle-reinforced composites.

Equation 2 shows that the hardness of the composites with harder particles is larger than the matrix hardness, H_m, and increases with particle volume fraction but decreases with particle size. The harder the particle, the higher the composite hardness.

It is clear from the Vickers hardness test that ageing influences properties of the composites. The T6 condition generally resulted in the highest hardness because of precipitate hardening compared to the other ageing conditions. An over-aged composite has a higher hardness than an under-aged one. On the other hand, it is indicated that the differential thermal contractions of the matrix and reinforcements enhanced the interfacial bonding and caused a higher dislocation density of the matrix [9]. In addition, variation in the type, shape, size and volume fraction of the particle reinforcements requires different peak-aged time. This is due to the different precipitation speeds of the hardening phases of different particles at the same ageing temperature. Equation 2 plays an important role in our wear rate analysis below.

3.2. Friction coefficient

3.2.1. Single-scratch tests

In single scratch tests, the average friction coefficient of five different materials under the T6 condition increased with increasing hardness as shown in Fig. 2 and Table II. It is clear that the hardness influences friction significantly. Fig. 3 shows the friction coefficients of 10% and 20% angular Al_2O_3–Al composites under three ageing conditions. When other factors, such as particle size and volume fraction, are unchanged, the increase of hardness by different heat treatments results in increasing friction coefficient. This is consistent with the frictional behaviour of most metals. However, the values of the friction coefficients of these composites are larger than those of metals predicted by Kopalinsky and Oxley [10] using slipline field theory because of different microstructures due to various particles and ageing conditions. Zhang *et al.* [11] indicated that the friction

TABLE I Vickers microhardness of the materials under three ageing conditions at an indentation load of 5 N

Materials	6061 Al alloy	6061 Al +10% SiC	6061 Al +20% SiC	6061 Al +10% Al_2O_3	6061 Al +20% Al_2O_3	Comral-85
UA	102 ±2	116 ±5	145 ±5	118 ±5	136 ±3	110 ±3
OA	108 ±2	122 ±5	150 ±5	125 ±5	139 ±3	112 ±3
T6	120 ±2	130 ±5	155 ±5	130 ±5	145 ±3	136 ±3

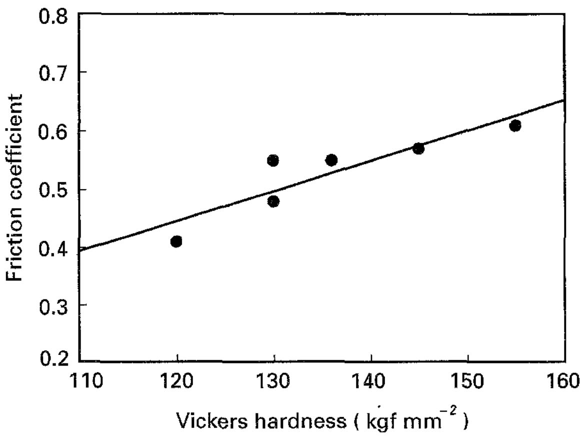

Figure 2 Variation of friction coefficient with the Vickers hardness of five materials under T6 conditions, at a normal load of 10 N.

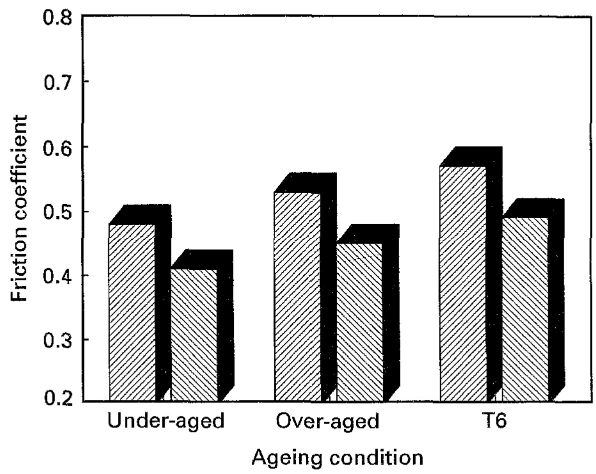

Figure 3 Friction coefficients of angular Al_2O_3–Al composites under three ageing conditions. ▧ 10% Al_2O_3; ▩ 20% Al_2O_3.

coefficient was composed of three terms: ploughing, adhesion and fracture of the particles. A frictional model was proposed to explain their relationships. Enhanced shear strength of the composites by reinforcements is one of the reasons for the resistance to scratching by the indentor. It can also be seen that a higher particle volume fraction leads to a higher hardness (see also Equation 2) and thus results in a larger friction coefficient. The particle size and type (with different hardness), on the one hand, influence the composite hardness as can be seen from Equation 2, in which the contribution of particle size d to $\bar{H}$ is less important than $\bar{H}_p$, and, on the other hand, affect the friction coefficient as indicated by Zhang *et al.* [11]. However, their relationship is not direct.

Fig. 4 shows that fluctuations existed although the mean friction coefficient was independent of sliding distance. Scratches on the other composites exhibited a similar behaviour. Such fluctuations were also observed in 6061 Al alloy, in which the groove width was uniform along the scratch. It is therefore reasonable to conclude that the fluctuations were mainly due to the natural stick–slip characteristics of friction, but not the particle reinforcements.

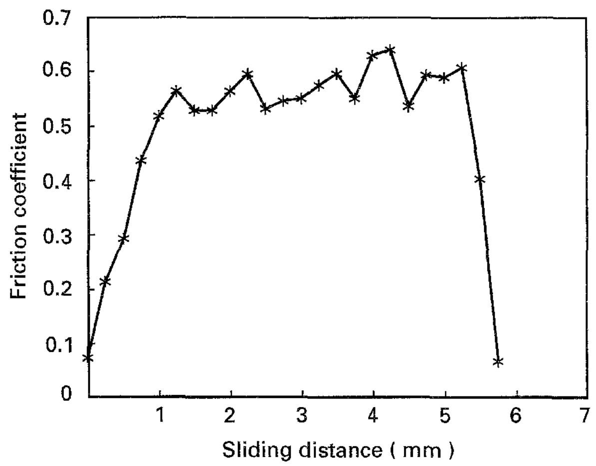

Figure 4 Relationship between friction coefficient and sliding distance in single-scratch tests on 10% SiC–Al composite with a diamond indentor.

3.2.2 Multiple-scratch tests

An actual wear process is so complex that only a single-scratch study is far from sufficient [9, 11, 13–16]. Therefore, multiple-pass scratches were arranged and carried out up to 10 passes by using a hard diamond indentor and a steel indentor with a Vickers hardness of 450 kgf mm^{-2}. A similar frictional behaviour was found in both cases. The friction coefficient was independent of pass number as shown in Fig. 5. Because of the reciprocating motion of the indentor, the frictional forces changed directions whenever the indentor moved backwards. Clearly, there was no noticeable difference of friction coefficient between single and multiple scratches. This implies that the three terms are still involved in the frictional process. Nevertheless, the proportion of each term is not necessarily the same as that in a single scratch. The adhesion term is expected to increase, and the ploughing term to decrease. However, further

TABLE II Particle size, Vickers hardness, friction coefficient and measured wear rate of the materials, at a load of 10 N under T6 condition

Materials	Diameter (μm)	Hardness, H_v (kgf mm^{-2})	Friction coefficient	Wear rate (10^{-6} mm^2)
6061 Al	0	120 ±2	0.41 ±0.03	710 ±10
10% SiC	1.8	130 ±5	0.55 ±0.08	600 ±12
20% SiC	1.8	155 ±5	0.61 ±0.05	565 ±12
10% Al_2O_3	4.5	130 ±5	0.48 ±0.05	652 ±15
20% Al_2O_3	8.8	145 ±3	0.57 ±0.04	594 ±15
Comral-85	18.7	136 ±3	0.55 ±0.04	628 ±15

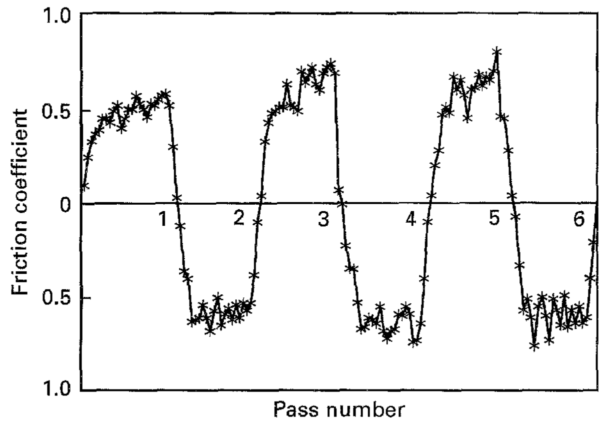

Figure 5 Variation of friction coefficient with pass number in multiple-scratch tests on 20% angular Al_2O_3–Al composite, at a normal load of 6 N using a diamond indentor.

complex tests (e.g. in the abrasive regimes in a pin-on-disc wear test) presented a much lower friction coefficient [17], indicating that the proportion of three terms changed or other factors may be involved in a real wear system, for example, the interaction of adjacent grooves, real contact numbers, various attack angles of the abrasives and the natural undulating surface. Therefore, the establishment of a quantitative relationship between the simple scratch tests and the complex pin-on-disc experiments needs further investigation.

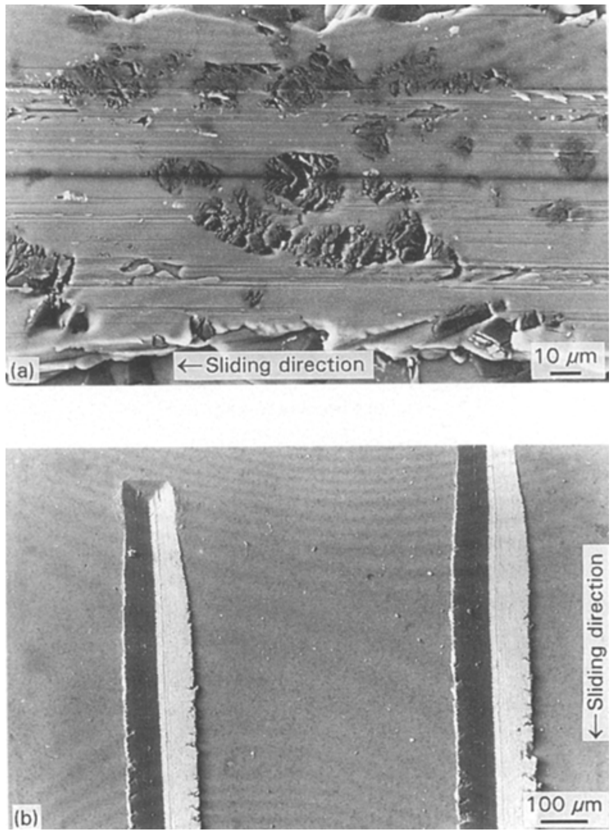

Figure 6 Groove topographies of (a) 20% angular Al_2O_3–Al composite, and (b) 20% SiC–Al composite.

3.3 Wear rate

3.3.1. Single scratch

In single-scratch tests, the groove size was constant with sliding distance in the tested load range. Therefore, wear rate, w, is defined as volumetric wear per sliding distance, i.e. the cross-sectional area of the groove measured by a laser confocal microscope. Under a normal load of 10 N, the material underneath the indentor is mainly cut or plastically deformed and there is little elastic deformation. The characteristics of the material along the scratch groove should be considered relative to a real wear situation. For example, are these loosened material or are they merely plastically deformed ridges? And how would the particles in the ridges behave? The wear rate in a single scratch does not necessarily describe the wear rate in a real application, because of its simplicity and idealization. Nevertheless, it provides some fundamental evidence for the abrasive wear phenomenon. Because of the differences in particle size and particle volume fraction of different composites, the topography of the grooves is different. Fig. 6a shows a rough groove ridge and worn surface of the composite reinforced with 20 vol% angular alumina particles with an average diameter of 8.8 μm. In this case, the particles beneath the indentor were fractured to debris which could not bear any load in the ensuing passes. In contrast, a very smooth and uniform groove on the surface of the composite reinforced with 20 vol% SiC particles with an average diameter of 1.8 μm was observed in Fig. 6b. Particle fracture is caused by the shear stress and lateral tensile stress applied on the particle. The crack is always at a certain angle with respect to the sliding direction, and a number of parallel cracks in each fractured particle can be seen in Fig. 6a. The smooth topography of SiC-reinforced composites in Fig. 6b is similar to that of 6061 Al alloy; this is because these composites contain such fine reinforced particles that the possibility of fracturing and debonding them is very small. The wear volume of this type of composite and unreinforced matrix is mainly determined by plastic deformation and cutting. Therefore, the hardness of the material is a dominant parameter affecting the wear rate, which is consistent with the observation by Rabinowicz [8] and Archard [12]. Archard's wear law is valid for composites with fine particles and gives the form

$$V = k\frac{PL}{H} \qquad (3)$$

where V is volumetric wear, k is a so-called wear coefficient, and L the sliding distance. Combining Equations 2 and 3, the volumetric wear can be obtained as

$$V = k\frac{PL}{H_m(1 + gf_v^{1.8}\bar{H}_p^{0.4}\bar{P}^{0.1})} \qquad (4)$$

It is clearly seen how these parameters influence the volumetric wear of the composites.

For large particle-reinforced composites, as discussed above, besides the hardness effect, particle fracture also plays an important role in determining the

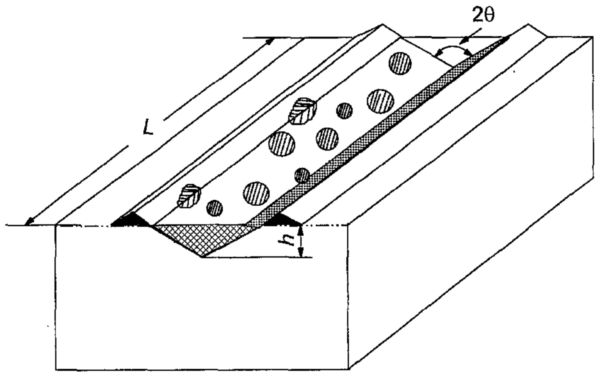

Figure 7 Schematic illustration of volumetric wear of the composite reinforced with spherical alumina particles.

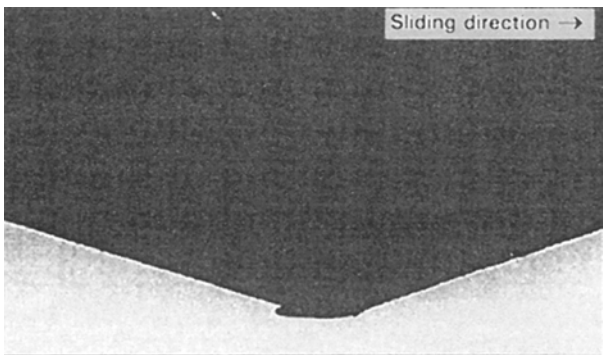

Figure 8 Wear of the steel indentor by a 20% angular Al_2O_3–Al composite after one pass.

wear rate. Fig. 7 shows schematically the scratched groove with ploughing, cutting or plastic deformation and fracture of large particles. The particle effect embraces the following aspects.

1. Increase of particle volume fraction results in higher hardness thus leading to higher friction coefficient and less wear rate
2. Large particle can resist the plastic strain efficiently and can reduce wear in cyclic sliding.
3. Particles in the matrix change the stress state under the sliding conditions and hence influence wear significantly.
4. Particles can be fractured by scratching with either the diamond or steel indentor. The fractured particle can be developed to a greater area with repeat sliding in the pin-on-disc test [17].
5. The rubbing pair can be worn out if its hardness is lower than that of the ceramic particle, see Fig. 8. Moreover, the difference of groove edges between composites with fine and coarse particles would result in different wear behaviour in real wear processes.

It follows from the above discussion that for all the composites studied, cutting or plastic deformation is always a dominant factor. However, particle fracture plays a significant role for composites with large particles. In other words, material hardness would most likely control the wear rate of composites reinforced with fine particle, but this would be altered to a great extent by particle fracture when the particles are relatively large. On the other hand, a ratio of the penetration depth to particle size is a very important parameter. When the ratio is less than unity, materials are difficult to be removed by the indentor, but if it is larger than unity, materials tend to be removed more easily. This is schematically illustrated in Fig. 9. Moreover, a higher volume fraction of the large reinforcement will increase the weight of particle fracture and, in turn, lead to a different wear behaviour. Table II demonstrates in detail the correlations between particle reinforcement, Vickers hardness, friction coefficient and the measured wear rates of 6061 Al alloy, SiC–Al composites and Al_2O_3–Al composites under the T6 condition.

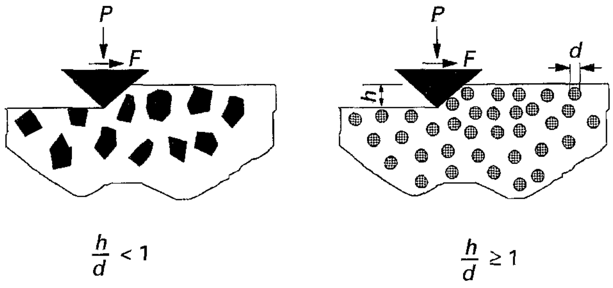

Figure 9 Illustration of material removal when the ratio h/d varies.

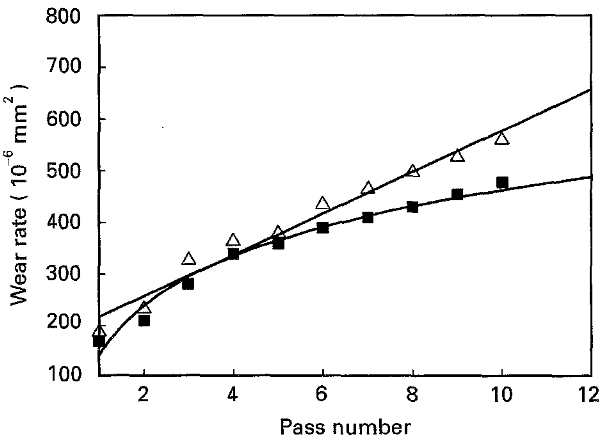

Figure 10 Variation of wear rate of a 20% spherical Al_2O_3–Al composite with pass number.

3.3.2. *Multiple scratches*

To explore correlation between scratch test and system wear, multiple scratches were also conducted. Koplinsky and Oxley [10] and Johnson [18] indicated that it is the accumulation of large plastic strain under cyclic sliding that causes the formation of wear particles. However, relatively large particles in the composites would change the stress state under the sliding surface. The larger the particle size, the more resistant to plastic strain and the lower the wear rate should be. On the other hand, the particles could also wear out the counterface such as steel. In this part of the study, a steel indentor with a Vickers hardness of 450 $kgf\,mm^{-2}$ was also used to compare with a diamond indentor.

The wear rate of the composites in multiple scratches by a diamond indentor differed to a great extent from that by a steel indentor, as indicated by the experimental results shown in Fig. 10. The increase in the composite wear rate by the diamond indentor is more pronounced with pass number than that by the steel indentor. This is due to the continuous wear of the steel indentor with increasing sliding distance. The wear rate of composites with large particles appeared to be smaller than that with smaller particles. In addition, composites at different ageing conditions have similar wear behaviour. It is apparent that the mechanical properties of the indentor materials play an important role. Because of the lower hardness of steel relative to the ceramic particles, the steel indentor was worn out in the first pass of scratches, Fig. 8. On the contrary, almost no wear was found on the hard diamond indentor even after 10 passes. The steel indentor becomes blunter with increasing pass number and thus its penetration and cutting ability was weakened. This result can be used to explain the considerable steel wear in a pin-on-disc test. Furthermore, multiple scratches by the steel indentor produced similar surface features and wear debris to those produced by pin-on-disc tests in the regime of abrasive wear [17]. Therefore, the relationship between scratch and pin-on-disc tests may be established after further systematic investigations.

4. Conclusions

The microhardness, friction coefficient and wear rate of MMCs with different heat-treatment conditions have been investigated. Based on the experimental observations, the following conclusions can be drawn.

1. The hardness of the composites can be expressed in a non-dimensional form

$$\bar{H} = 1 + gf_{\mathrm{v}}^{1.8}\bar{H}_{\mathrm{p}}^{0.4}\bar{P}^{0.1}$$

2. Increase of hardness by larger volume fraction of particles or different ageing conditions increases the friction coefficient and reduces the wear rate. Compared to other ageing conditions, peak-aged composites have the best wear resistance but the largest friction coefficient.

3. The wear rate of a composite with fine particles is mainly affected by its hardness, but that of large particle-reinforced composites depends on the ratio of the penetration depth to the particle size.

4. Composites with large particles cause remarkable steel wear in a single scratch, thus large particles would accelerate the steel wear in a wear system.

Acknowledgements

The authors thank the Australian Research Council for the continuing support of this work, and Comalco Research Centre in Thomastown, Victoria for supplying the MMC materials for testing. The Electron Microscopy Unit of the University of Sydney provided access to its facilities. Z. F. Zhang is supported by an EMSS scholarship.

References

1. A. G. WANG and H. J. RACK, *Wear* **146** (1991) 337.
2. Z. Y. MA, J. BI, Y. X. LIU, H. W. SHEN and Y. X. GAO, *ibid.* **148** (1991) 287.
3. Z. F. ZHANG, Y. X. CHEN, A. K. MUKHOPADHYAY and Y.-W. MAI, in MMC-3, "Proceedings of the 3rd Australian Forum on Metal Matrix Composites", edited by S. Bandyopadhyay and A. G. Crosky (University of New South Wales, Sydney, 1992) pp. 63–73.
4. C. BADINI, F. MARINO and A. TOMASI, *Mater. Sci. Eng.* **A 136** (1991) 99.
5. H. L. LEE, W. H. LIEU and S. L. CHAN, *Wear* **159** (1992) 223.
6. S. J. LIN and K. S. LIU, *ibid.* **121** (1988) 1.
7. A. T. ALPAS and J. D. EMBURY, "Wear of materials" (ASME, New York, 1985) pp. 784–93.
8. E. RABINOWICZ, "Friction and wear of materials" (Wiley, New York, 1965).
9. K. H. ZUM GAHR, "Microstructure and wear of materials", Tribology Series 10 (Elsevier, Amsterdam, 1987).
10. E. M. KOPALINSKY and P. L. B. OXLEY, in "Proceedings of the 4th International Tribology Conference", AUSTRIB'94, edited by G. W. Stachowiak, Vol. 1 (UNIPRINT, University of Western Australia, Perth, 1994) pp. 33–34.
11. Z. H. ZHANG, L. C. ZHANG and Y-W. MAI, *Wear* **176** (1994) 231.
12. J. F. ARCHARD, *J. Appl. Phys.* **24** (1953) 981.
13. A. J. SEDRIKS and T. O. MULHEARN, *Wear* **6** (1963) 457.
14. C. A. BROOKES, P. GREEN, P. H. HARRISON and B. MOXLEY, *J. Phys. D Appl. Phys.* **5** (1972) 1284.
15. J. A. WILLIAMS and Y. XIE, *Wear* **155** (1992) 363.
16. B. R. LAWN, *ibid.* **33** (1975) 369.
17. Z. F. ZHANG, L. C. ZHANG and Y.-W. MAI, *J. Mater. Sci.* (1994) in press.
18. K. L. JOHNSON, in "Proceedings of the 4th International Tribology Conference", AUSTRIB'94, edited by G. W. Stachowiak, Vol. 1 (UNIPRINT, University of Western Australia, Perth, 1994) pp. 53–58.

Received 12 January
and accepted 7 June 1995